Science of the Total Environment 807 (2022) 151081

Contents lists available at ScienceDirect

Science of the Total Environment

journal homepage: www.elsevier.com/locate/scitotenv

# Temporal variation in $TiO_2$ engineered particle concentrations in the Broad River during dry and wet weathers

Md Mahmudun Nabi [a], Jingjing Wang [a], Erfan Goharian [b], Mohammed Baalousha [a,*]

[a] Center for Environmental Nanoscience and Risk, Department of Environmental Health Sciences, Arnold School of Public Health, University of South Carolina, SC 29208, USA
[b] Department of Civil and Environmental Engineering, University of South Carolina, SC 29208, USA

## HIGHLIGHTS

- The concentration of $TiO_2$ engineered particles in the Broad River was estimated.
- Elemental composition of Ti-particles was characterized on a single particle basis.
- The concentration of $TiO_2$ engineered particles correlated linearly with turbidity.
- The correlation between $TiO_2$ and turbidity varied with flow regime.
- The elemental ratio of Ti/Fe in Ti-bearing particles increased with increases in pH.

## GRAPHICAL ABSTRACT

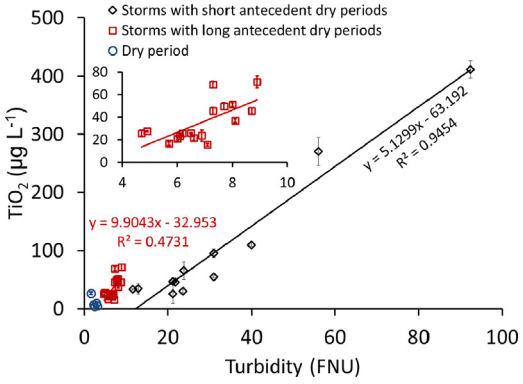


## ARTICLE INFO

*Article history:*
Received 10 September 2021
Received in revised form 14 October 2021
Accepted 15 October 2021
Available online 20 October 2021

Editor: Damià Barceló

*Keywords:*
TiO2
Engineered particles
Turbidity
SP-ICP-TOF-MS
Elemental ratios
Linear correlation

## ABSTRACT

Titanium dioxide ($TiO_2$) engineered particles are widely used in the urban environment as pigments in paints, and as active ingredients in photocatalytic coatings. Consequently, studies are necessary to quantify $TiO_2$ engineered particle concentrations and their temporal variability in surface waters to gain better understanding about their abundance and environmental fate in order to minimize their potential environmental impacts. The objective of this study was to determine the temporal variability in the concentration of $TiO_2$ engineered particles in the Broad River, Columbia, South Carolina, United States during dry and wet weather conditions and to examine the relationship between flow discharge, water quality indicators, and the concentration of $TiO_2$ engineered particles. $TiO_2$ engineered particle concentration in the Broad River water was determined by mass balance calculation using bulk titanium concentration and the increase in Ti/Nb ratio above the natural background ratio. The relative abundance of single metal and multi-metal Ti-bearing particles was determined by single particle-inductively coupled plasma-time of flight-mass spectrometer (SP-ICP-TOF-MS). Additionally, the elemental ratios of Ti/Nb, Ti/Al, and Ti/Fe within multi-metal Ti-bearing particles were determined at the single particle level. Discharge, bulk elemental concentrations (*e.g.*, Ti, Al, Fe, and Nb), bulk elemental ratios (*e.g.*, Ti/Al, Ti/Fe, and Ti/Nb), $TiO_2$ engineered particle concentration, and turbidity displayed the same trend of rise and fall following storm events. Linear relationships were established between turbidity and $TiO_2$ engineered particle concentrations in the Broad River for different flow regimes. However, no correlation was observed between $TiO_2$ engineered particle concentrations and flow discharge, dissolved oxygen, pH, or ionic strength. The established correlations between turbidity and $TiO_2$ engineered particle concentrations are important as they can be used to translate the continuously monitored turbidity to $TiO_2$ concentrations.



* Corresponding author.
*E-mail address:* mbaalous@mailbox.sc.edu (M. Baalousha).

https://doi.org/10.1016/j.scitotenv.2021.151081
0048-9697/

## 1. Introduction

Field data on the temporal variability in titanium dioxide ($TiO_2$) engineered particle concentrations in urban surface waters during and after storm events remains scarce, despite the wide use of $TiO_2$ engineered particles in the urban environment as pigments (*e.g.*, 100–300 nm) and as engineered nanoparticles (*e.g.*, 1–100 nm) in self-cleaning surfaces (Baalousha et al., 2016). For instance, paint, which contain up to 10% $TiO_2$ particles, demand is estimated at 5.3 billion liters $year^{-1}$ in 2019 in the United States, a third of which (*e.g.*, 1.77 billion liters) is used for exterior paint (Coatingsworld, 2019). These uses of $TiO_2$ engineered particles result in their release and deposition on surfaces in the urban environment which later can be washed off by rainfall and surface runoff (Wang et al., 2020). Consequently, several studies identified $TiO_2$ engineered particles in urban media such as fine and ultrafine atmospheric particulate matter (Wilczyńska-Michalik et al., 2015), dust dry deposition (Lee et al., 2016), road dust, sludge from storm drains, and roadside soils (Adamiec, 2017), bridge runoff (Wang et al., 2020), rain and surface water (Azimzada et al., 2021; Wang et al., 2022), and stormwater green infrastructure (Baalousha et al., 2020). Most studies reported the occurrence, without providing estimated concentrations, of $TiO_2$ engineered particles in environmental samples based on measuring total Ti concentrations and identifying few particles in a given sample using transmission electron microscopy (TEM) (Lee et al., 2016; Wilczyńska-Michalik et al., 2015). Other studies estimated the concentrations of $TiO_2$ engineered particles in environmental samples based on environmental fate modeling (Gottschalk et al., 2013; Parker and Keller, 2019). Nonetheless, recent studies reported quantitative measured concentrations of $TiO_2$ engineered particles in environmental samples such as sewage spills (Loosli et al., 2019), stormwater runoff (Wang et al., 2020), stormwater green infrastructure (Baalousha et al., 2020), and surface water (Azimzada et al., 2021; Nabi et al., 2021a; Wang et al., 2022). These studies focused on developing approaches to detect and quantify $TiO_2$ engineered particle concentrations in environmental samples and did not investigate the event-scale temporal variability or the relationship between $TiO_2$ engineered particle concentrations and environmental parameters such as flow discharge, temperature, pH, dissolved oxygen, turbidity, or suspended solids.

In most cases, contaminant, including $TiO_2$ engineered particle, in urban rivers are not characterized by a constant concentration, but rather by the episodic or random occurrence of rainfall events, snowmelt, and/or return flows and subsequent high river flows (Nabi et al., 2021a). For instance, a recent environmental fate modeling study suggested that stormwater runoff could result in high variability in $TiO_2$ engineered nanoparticle concentrations in urban rivers, with high flow events generating a large proportion of the total annual $TiO_2$ engineered nanoparticle loads in rivers (Parker and Keller, 2019). Variables affecting contaminant load in rivers, thus may affect $TiO_2$ engineered particle concentrations, include antecedent rainfall, duration of the rainfall event, rainfall intensity of the event, succession of rainfall events, time of rise and fall of the hydrograph, runoff duration, peak discharge and total runoff (Onderka et al., 2012). Between rainfall events, contaminants in the catchment, including $TiO_2$ engineered particles, tend to build up *via* dust blown in by wind, tire wear residue, paint and road marking wear, *etc*. Thus, the longer period between the antecedent and current rainfall events, the greater the mass of an individual contaminant available for wash-off from surfaces in the basin. In response to the changing intensity, duration, and frequency of rainfall events, some or all the available contaminants are washed off and transported to receiving surface waters (Vercruysse and Grabowski, 2019; Vercruysse et al., 2017). While the contaminant mass can increase by storm events, higher peak flows and discharges may end up displaying lower concentrations due to dilution effects.

This study aims to (1) quantify the temporal variability in $TiO_2$ engineered particle concentrations in the Broad River, Columbia, South Carolina, United States during dry and wet weather conditions under rainfall events of various characteristics, (2) evaluate the impact of rainfall events characteristics on $TiO_2$ engineered particle concentrations, and (3) determine the correlation between $TiO_2$ engineered particle concentrations, flow discharge, and environmental indicators with particular emphasis on turbidity as a surrogate for suspended sediment concentration.

## 2. Materials and methods

### 2.1. Sampling site

The Broad River is a principal tributary of the Congaree River, about 240 km long in western North Carolina and northern South Carolina in the Unites States. The Broad River originates in the Blue Ridge Mountains of eastern Buncombe Country, North Carolina, and flows generally south-southeastwardly, through or along the boundaries of Rutherford, Polk, and Cleveland Counties in North Carolina, and Cherokee, York, Union, Chester, Fairfield, Newberry, and Richland Counties in South Carolina. The broad River joins the Saluda River near the City of Columbia in South Carolina to form the Congaree River. The total drainage area of the Broad River is approximately 14,035 $km^2$ (SCdhec, 2007). Land use throughout the Broad River basin is a mix of commercial and residential properties with agricultural (row crops and pasture) and forested land in the headwaters. There are permitted 14 major waste water treatment plants (WWTP), 30 minor WWTPs, 20 animal operation facilities, 92 general and individual stormwater facilities in the Broad river basin (SCdhec, 2007).

Water samples were collected from the Broad River, Columbia, SC 29201 (34°00′10.4″N 81°03′18.4″W) during a range of hydrologic settings including wet weather conditions with different rainfall intensities and during a dry period (Table S1). The period March 2019 to April 2019 experienced typical rain conditions in Columbia, South Carolina, United States with average rainfall of approximately 50 to 100 mm per month, whereas the period of August to September 2019 experienced dry condition with average rainfall of <25 mm per month, majority of which occurred during the month of September (CPC). The precipitation data was collected from the United States Geological Survey (USGS) gauge station number 021695045 (34°00′24″N 81°01′18″W), nearly 3.5 km from the water sampling location. The flow discharge data also was collected from the USGS, station number 02162035 (34°02′54″N 81°04′24″W), which is located nearly 4.5 km upstream of the sampling location (Fig. S1).

### 2.2. Sampling site and elemental analysis

Water samples were collected from the Broad River, Columbia, SC 29201 (34°00′10.4″N 81°03′18.4″W) in a 1 L high-density polyethylene bottles (Thermo Scientific, Rockwood, TN, United States). Prior to use, bottles were soaked in 10% nitric acid (Acros Organics, Czech Republic) for at least 24 h followed by soaking in ultrapure water (UPW, PURELAB Option-Q, ELGA, UK) for 24 h, air dried, and then double-bagged. In the field, the sampling bottles were rinsed three times in the surface water before filling with the water sample. Samples were individually double-bagged and returned to the lab the same day, where they were stored at 4 °C in the dark until further analysis. All samples were digested with HF:$HNO_3$ (3:1) mixture (ACS grade acids distilled in the laboratory) and analyzed for total elemental concentrations using Perkin Elmer NexION 350D ICP-MS according to the protocols described in detail in elsewhere (Loosli et al., 2019; Nabi et al., 2021a). The method limit of detection and quantification are summarized in Table S2.

### 2.3. Hydrograph separation

In order to estimate the flow contribution of the storm, first the baseflow (dry flow) should be separated from the direct runoff of the

storm event. The baseflow in a river is often attributed to the gradual snowmelt, groundwater discharge to the river, or urban or agricultural return flow to the river. The direct runoff in a river is the portion of the total discharge that is produced by rainfall. In this study, we used the Web based Hydrograph Analysis Tool (WHAT) (Lim et al., 2005) to separate the total discharge to direct runoff and baseflow.

### 2.4. Calculation of total $TiO_2$ engineered particle concentration

The concentration of $TiO_2$ engineered particles in the river water was calculated according Eq. 1 assuming that all Ti occur in particulate form, that Nb occurs only in natural Ti-bearing particles with constant Ti/Nb ratio, that anthropogenic Ti occur as pure $TiO_2$ particles (Gaspar and Wyllie, 1983; Gondikas et al., 2014; Loosli et al., 2019; Nabi et al., 2021a; Nakashima and Imaoka, 1998).

$$[TiO_2]_{engineered\ particles} = \frac{TiO_{2\ MM}}{Ti_{MM}}\left[Ti_{sample} - Nb_{sample}\cdot\left(\frac{Ti}{Nb}\right)_{background}\right] \quad (1)$$

where, $[TiO_2]_{engineered\ particles}$ is the concentration of $TiO_2$ engineered particles, $Ti_{\ MM}$ and $TiO_{2\ MM}$ are the molar masses of Ti and $TiO_2$, $Ti_{sample}$ and $Nb_{sample}$ are the concentrations of Ti and Nb in a given sample, $Ti/Nb_{background}$ is the natural background elemental concentration ratio of Ti/Nb. Background Ti/Nb ratio was calculated on eight reference samples collected from Lake Katherine and Gills creek in Columbia, SC in the absence of rainfall events (Loosli et al., 2019). Elemental ratios (*e.g.*, Ti/Nb) have been recently implemented to quantify the total concentration of $TiO_2$ engineered particles in wastewater treatment plants (Nabi et al., 2021b), urban runoff (Wang et al., 2020), stormwater green infrastructure (Baalousha et al., 2020), surface waters (Loosli et al., 2019; Nabi et al., 2021a).

### 2.5. Multi-element single particle analysis

The water samples were shaken vigorously prior extraction to avoid particle losses by sedimentation and to obtain a representative subsample. Ten mL aliquots were transferred into acid-washed 15 mL centrifuge tubes (Fisher Scientific, San Nicolás de los Garza, Nuevo León, Mexico). The transferred samples were bath sonicated for 2 h (Branson, Model 2800, 40 kHz, Danbury, CT, United States), then centrifuged at 775*g* for 5 min (Eppendorf Centrifuge 5810R, Hamburg, Germany) to remove large particles (>1000 nm, assuming natural particle density $\rho = 2.5\ g\ cm^{-3}$) to prevent clogging of the ICP-TOF-MS introduction system. The top 7 mL supernatant was decanted and stored at 4 °C in the dark till analysis by SP-ICP-TOF-MS. The theoretical size of the extracted fractions corresponds to particles <725 nm for $TiO_2$ particles ($\rho = 4.2\ g\ cm^{-3}$). All samples were bath sonicated again for 15 min immediately prior to SP-ICP-TOF-MS analysis. All samples were diluted 100 folds in ultrapure water prior to the analysis. The Ti recovery of the particle extraction method was calculated as the total mass of Ti single particles to the total mass of Ti in the bulk water samples and varied between 1.6 and 11.2%.

Single particle analysis was performed using an ICP-TOF-MS (TOFWERK, Thun, Switzerland) to determine all isotopes within a single particle simultaneously (Hendriks et al., 2017). Element specific instrument sensitivities were measured with a multi-element solution mix prepared from a multi-element solution (0, 1, 2, 5, and 10 $\mu gL^{-1}$ multi element standard, diluted in 1% $HNO_3$, BDH Chemicals, Radnor, PA, USA). The transport efficiency was calculated *via* the known size approach (Pace et al., 2011) using both Au ENMs with a certified particle size of 60 nm (NIST RM8013 Au, Gaithersburg, MD, USA) and Au standard solutions (0, 1, 2, 5, and 10 $\mu gL^{-1}$, diluted in 1% HCl, BDH Chemicals, West Chester, PA, USA) prepared in UPW. Using a standard tuning solution, the ICP-TOF-MS mass spectra were calibrated using $^{18}H_2O^+$, $^{59}Co^+$, $^{115}In^+$, $^{140}Ce^+$, and $^{238}U^+$ target isotopes in TofDAQ view. Particle/baseline signal separation, particle signals, particle mass, and particle number concentration were determined from mass-calibrated ICP-TOF-MS spectra using Python script in Tofware as described elsewhere (Loosli et al., 2019). The data for each isotope were treated separately, but the time stamps were kept throughout data processing for every isotope, allowing for identification of isotope correlations in a single particle. The elemental mass detection limit for SP-ICP-TOF-MS analysis is summarized in Table S2. Procedural blanks were analyzed together with the samples. Only 15 Ti spikes were detected in the procedural blanks corresponding to a particle number concentration of $3.20 \times 10^4$ Ti-bearing particles $L^{-1}$ and a total particle mass concentration of $1.21 \times 10^{-4}$ μg $L^{-1}$, which are negligible compared to those measured in the river water samples (see Results and discussion).

## 3. Results and discussion

### 3.1. Rainfall-runoff characteristics

Five rainfall events were monitored during the period 03/20/2019 to 04/19/2019 (Table S1) in addition to a dry period (09/23/2019 to 09/27/2019). Rainfall intensity varied from 0.25 to 28 mm $day^{-1}$. The antecedent dry days (ADD) varied from 0 to 15 days. The two rainfall events between 03/20/2019 and 04/04/2019 were characterized by relatively long ADDs (7 and 15 days), whereas the rainfall events between 04/05/2019 and 04/19/2019 were characterized by short ADDs (0 to 2 days). Among these 5 rainfall events, only the last two events lasted for more than a day, while the duration of the rainfalls on March 25th, April 2nd and 5th was less than a day. The heaviest rainfall event occurred on April 2nd (28.2 mm per day), followed by the rainfall during the first day (April 12th) of the last event, and the rainfall event on April 5th event. In general, higher intensity of rainfall happens during the less frequent and shorter duration of storm events.

The events' hydrograph and time series of river discharge at the Broad River show that the river's flow regime is highly sensitive to the storms and reaches to its peak value in a short period during the rainfall events, *i.e.* the basin's time of concentration and time of peak is relatively small (Fig. 1). The river's discharge between 04/07/2019 and 04/17/2019 was higher than that between 03/20/2019 and 04/06/2019 and during the drought period between 09/23/2019 and 09/27/2019. This is because rain events between 04/05/2019 and 04/19/2019 were preceded by short antecedent dry periods, whereas those between 03/20/2019 and 04/04/2019 were preceded by longer antecedent dry periods (Table S1). Antecedent meteorological and hydrogeological conditions determine the hydrological response of a basin, as the smaller ADD

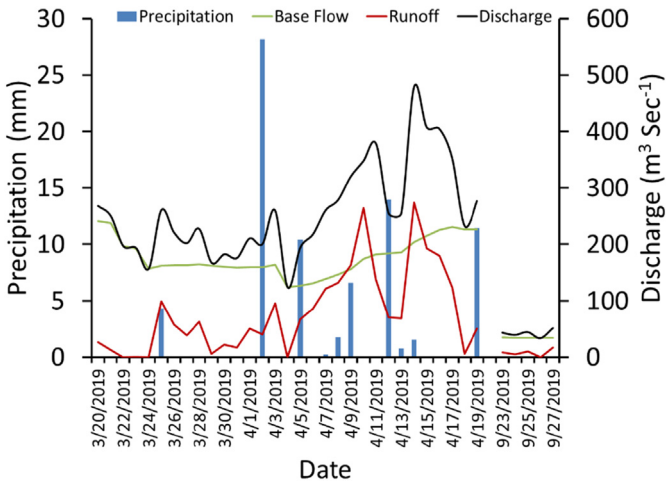


**Fig. 1.** Hydrological conditions during the sampling period. March to April was wet weather period, whereas, September was drought conditions.

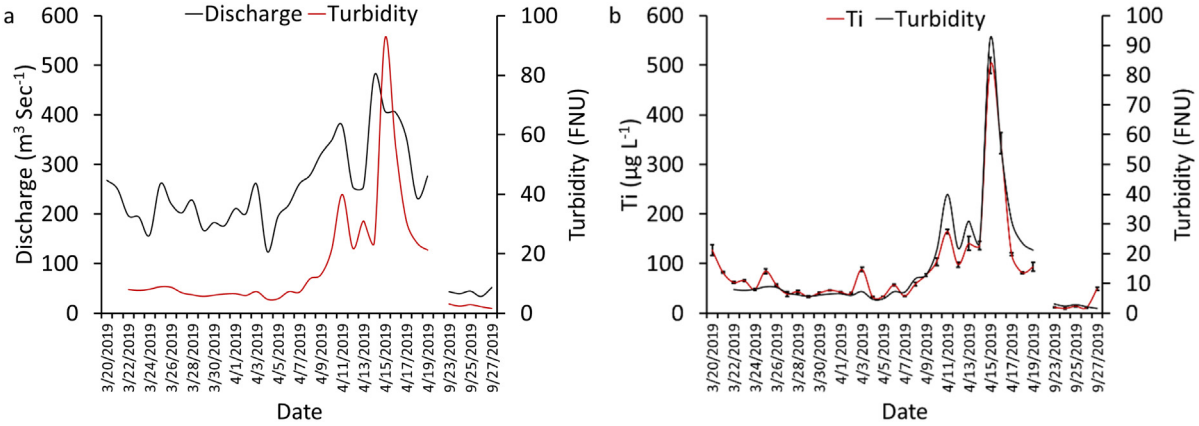


**Fig. 2.** Hydrograph and pollutographs (a) discharge-turbidity relationship, (b) Ti concentration-turbidity relationship. FNU: formazin nephelometric units.

means higher soil moisture in the basin and less capacity of infiltration during the next storm (Onderka et al., 2012; Vercruysse et al., 2017). Thus, under dry conditions, the water storage capacity of a catchment is higher than under wet conditions when the surface and subsurface storage are likely to be saturated. As the pore size fills with water, the infiltration capacity of the soil profile decreases. Any additional rainfall occurring after soil saturation becomes runoff immediately, even if the rainfall intensity is very small (Istok and Boersma, 1986). Thus, rainfall events of similar magnitudes, but different ADD and soil moisture, can result in runoffs of different magnitudes. Moreover, the evapotranspiration rates are lower during the wet seasons. These collectively result in higher runoff following rainfall events during wet conditions, while rainfall events during dry conditions produce low runoff amounts, or may not produce any measurable runoff, unless if the intensity of rainfall is significant (Istok and Boersma, 1986; Penna et al., 2011).

### 3.2. Time-flow-concentration trend plots

The temporal variability in pollutant concentration was observed through time-flow-concentration graphs (hydro-pollutographs, Fig. 2). The hydrograph and the pollutographs show similar trend of rise and fall of discharge and pollutant concentrations following rainfall events. The major water quality change that occurred during wet-weather events was the substantial increase in turbidity, the other water quality indicators such as temperature, dissolved oxygen, and pH were not sensitive to the changes in flow (Figs. 2a, S2). Turbidity values measured

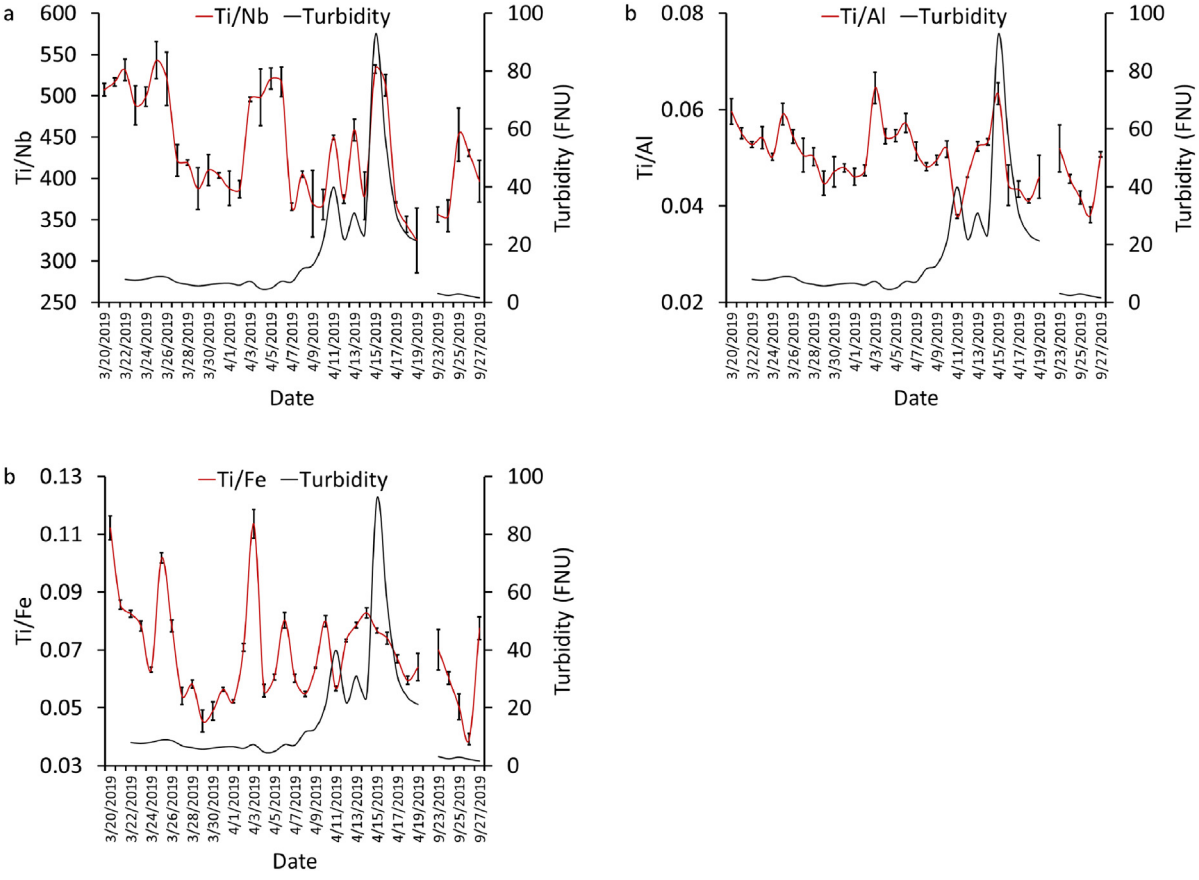


**Fig. 3.** Elemental ratio as a function of time (a) Ti/Nb, (b) Ti/Al, and (c) Ti/Fe.

between 04/10/2019 and 04/19/2019 were higher than those measured between 03/20/2019 and 04/09/2019 and during the dry period 09/23/2019 to 09/27/2019. Increased turbidity regularly occurs during rain events when rainfall and runoff mobilize particles from the riparian zone, upstream locations in the watershed, and the overall stream network within a basin (Chen and Chang, 2014). Water from rain events and related runoff increase discharge and flow velocity, which in turn, increase shear stress and turbulence, and therefore increase sediment erosion and transport.

Fig. 2a shows that equal peaks of discharge may have different magnitude of turbidity. For example, the peak on 04/09/2019 (264 $m^3$ $sec^{-1}$; 40 FNU) and 04/15/2019 (274 $m^3$ $sec^{-1}$; 92 FNU), which can be attributed to variability in suspended sediment concentrations during storm events. Many studies found that turbidity in river waters during rainfall events exhibits close positive correlation with suspended sediment concentrations (Lewis, 1996; Patil et al., 2011), and thus many studies used turbidity as a surrogate of suspended sediment loadings in rivers and streams (Chanson et al., 2008; Mosbrucker, 2014; Uhrich and Bragg, 2003; Wass et al., 1997).

The increases in Ti concentrations coincided (timewise) with increases in turbidity (Fig. 2b), but not with discharge (Fig. 2a). All other elements (*e.g.*, Nb, Al, and Fe) followed the same trend with slight variations in the concentrations during different rain events (Fig. S3). These results suggest that suspending sediments is the key driver of metal mobility during rainfall events. Numerous studies reported elemental concentrations to estimate pollution loads during runoff events (Hussain et al., 2017; Sakson et al., 2018). However, metals may have both natural as well as anthropogenic origins. Metals occur naturally in soils, which is one of the primary sources of suspended sediments. Soil particles are also important constituent of urban dust, thus they are a significant contributor to metal flow into rivers during runoff events. Therefore, elemental concentrations do not allow differentiating natural from anthropogenic contributions.

### 3.3. Time-dependent elemental ratios

The elemental ratios of Ti/Nb, Ti/Al, and Ti/Fe show similar trend of rise and fall following rainfall events to each other and to turbidity (Fig. 3). The elemental ratio of Ti/Nb varies between 324.8 ± 39.5 (4/19/2019) and 543.2 ± 22.5 (3/25/2019). The elemental ratio of Ti/Al varies between 0.038 ± 0.002 and 0.065 ± 0.003. The elemental ratio of Ti/Fe varies between 0.039 ± 0.002 and 0.114 ± 0.005. The lowest Ti/Al and Ti/Fe occurred on 9/26/2019 and the highest Ti/Al and Ti/Fe occurred on 4/03/2019. These elemental ratios were generally higher than the natural background elemental ratios, indicating Ti-particle contamination. For instance, the Ti/Nb, Ti/Al, and Ti/Fe ratios were generally higher than the reference ratios (*e.g.*, 267 ± 8.9, 0.049 ± 0.003, and 0.037 ± 0.005, respectably) measured in smaller creeks in the sampling area (Loosli et al., 2019), and higher than the average crustal ratios (*e.g.*, 320, 0.049, and 0.1 respectively) (Rudnick et al., 2003). The increase in the elemental ratios coincided with the increase in the turbidity, suggesting that turbidity (*e.g.*, suspended solids) is the key factor driving the increase in elemental ratios due to anthropogenic particulate Ti contamination.

The concentration of $TiO_2$ engineered particles were estimated based on Ti/Nb, Ti/Al, and Ti/Fe (Fig. 4a). The concentration of $TiO_2$ engineered particles follow the same trend using the three elemental ratios, suggesting that these three elemental ratios can be implemented to estimate of $TiO_2$ engineered particle concentrations in this study. However, some differences are observed between the estimated $TiO_2$ engineered particle concentrations, which might be attributed to the unique associations and behaviors of these elements within natural Ti-bearing particles (see further discussion in Section 3.3). Although Nb, Fe, and Al occur in natural Ti-bearing particles and can be used as tracers (Loosli et al., 2019), Nb is the only element that is exclusively associated with Ti (Baalousha et al., 2021). On the other hand, Fe- and Al-bearing

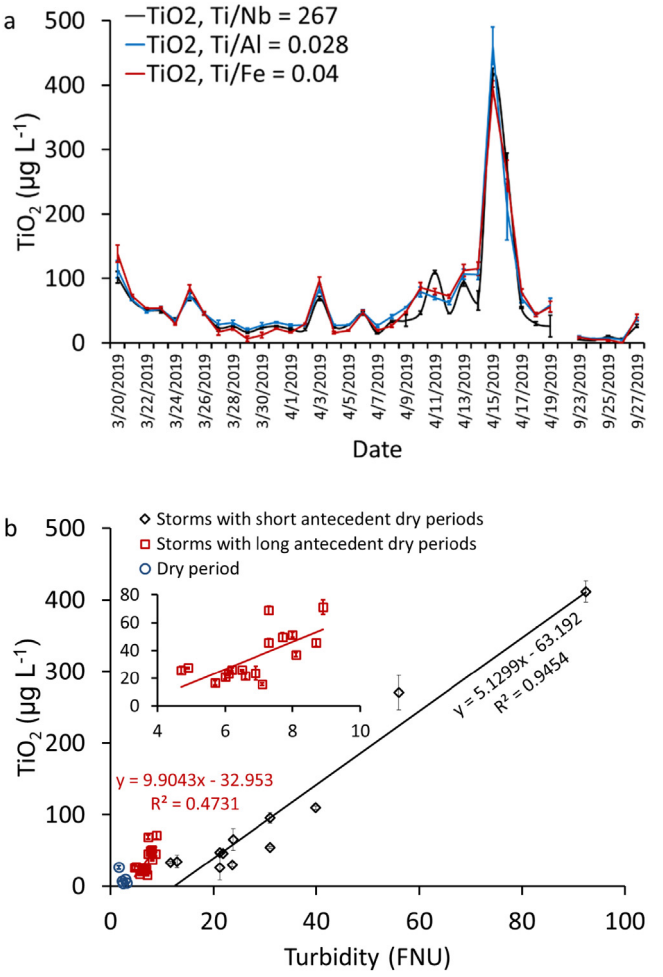


**Fig. 4.** (a) $TiO_2$ concentrations estimated based on Ti/Nb, Ti/Al and Ti/Fe elemental ratios, and (b) Correlation between $TiO_2$ concentrations estimated based on Ti/Nb and turbidity. $Ti/Nb_{bg}$, $Ti/Al_{bg}$, and $Ti/Fe_{bg}$ refers to the natural background elemental ratios.

particles occurred both as single metal particles and as particles associated with Ti-bearing particles (Baalousha et al., 2021). Thus, Ti/Nb most likely provides the most accurate estimate of $TiO_2$ engineered particle concentrations.

### 3.4. Turbidity-$TiO_2$ relationship

In general, increases in turbidity resulted in increases in $TiO_2$ concentration (Fig. 4b). However, three different associations can be identified. During the dry season both turbidity and $TiO_2$ concentration were low. During the wet season, a strong ($R^2$ of 0.94) linear relationship was established between turbidity and $TiO_2$ concentration for rainfall events that were preceded with short antecedent dry periods, and a weaker ($R^2$ of 0.47) linear relationship was established between turbidity and $TiO_2$ concentration for rainfall events that were preceded with long antecedent dry periods. These findings suggest that turbidity can be used as a substitute to predict $TiO_2$ concentrations within this watershed. However, as shown here, this relationship depends on several factors such as antecedent dry periods and is likely to be site specific. It is worth noting that a strong positive relationship was observed between total suspended solid concentration and turbidity in rivers, which varied for a particular catchment and within a particular period (Daphne et al., 2011; Packman et al., 1999; Sun et al., 2001). This variation between turbidity and suspended sediment underpins our observation of the

variation between turbidity and $TiO_2$, given that $TiO_2$ is typically associated with suspended solids.

### 3.5. Characterization of Ti-bearing particles by SP-ICP-TOF-MS

The number concentration of all, single metal, and multi-metal Ti-bearing particles, determined by SP-ICP-TOF-MS, display a similar trend of rise and fall following rainfall events as the $TiO_2$ engineered particle mass concentrations (Fig. 5a). Approximately, 29 to 83%, (Fig. 5b) of Ti-bearing particles were single metal, that is based on icp-TOF-MS analysis results that these particles did not contain any natural tracers. This can be due to either (1) these single metal Ti-bearing particles are pure $TiO_2$ engineered particles, and/or (2) the concentrations of natural tracers in these single metal Ti-bearing particles are below the SP-ICP-TOF-MS size detection limit (Baalousha et al., 2021). The remaining particles (*e.g.*, 17–71%) contained at least one natural tracer such as Fe, Al, Si, Zr, Nb, Th, Ce, Ba, Mn, Pb, Ni, Zn, La, V, U, Ta, Cr, and W, indicating that these particles are most likely naturally occurring particles. This is in good agreement with elemental association between Ti and other elements in natural surface waters and soils in South Carolina, United States (Baalousha et al., 2021; Loosli et al., 2019). This is also in good agreement with the impurities (*e.g.*, Nb, Ta, Sb, W, V, Cr, Mo, and Sn, Zr, Fe, U and Pb) detected in natural $TiO_2$ minerals (such as rutile and ilmenite) (Gaspar and Wyllie, 1983; Nakashima and Imaoka, 1998; Zack et al., 2002).

The relative abundance of single metal Ti-bearing particles also displays the same trend of rise and fall following rainfall events as the $TiO_2$ engineered particle concentrations (Fig. 5b). It is worth noting that Nb always occurred in association with Ti-bearing particles, whereas all other natural tracers occurred both in association with Ti-bearing particles and in single metal particles form. This is because Ti and Nb occur in natural titanium minerals such as rutile, anatase, sphene, and/or opaque heavy minerals (*e.g.*, titanomagnetite, magnetite, and ilmenite) (Craigie, 2018). Natural $TiO_2$ minerals, such as rutile and ilmenite, have been shown to be the dominant carrier (*e.g.*, >90–95% of the whole rock content) for Ti, Nb, Ta, Sb, and W as well as an important carrier (*e.g.*, 5–45% of the whole rock content) for V, Cr, Mo, and Sn in $TiO_2$-bearing metamorphic rocks (Gaspar and Wyllie, 1983; Zack et al., 2002).

The relative abundance of single metal particles was higher during the high runoff periods (*e.g.*, 04/11/2019 to 04/19/2019) than those during the low runoff events (*e.g.*, 03/23/2019 to 04/10/2019) and the drought period (*e.g.*, 09/23/2019 to 09/27/2019). These findings indicate the increase in the relative abundance of single metal particles during runoff events can be attributed to $TiO_2$ engineered particles in the runoff.

The elemental ratios of Ti/Al, Ti/Fe, and Ti/Nb, determined on single particle basis, display the same trend in all samples. Most particles exhibited Ti/Al ratio within the range 0 to 0.4 (72 to 98%, Fig. 6a), Ti/Fe ratio within the range 0 to 2.0 (75 to 95%, Fig. 6b), and Ti/Nb ratio within the range 0 to 400 (97 to 100%, Fig. 6c). Nonetheless, a small fraction of

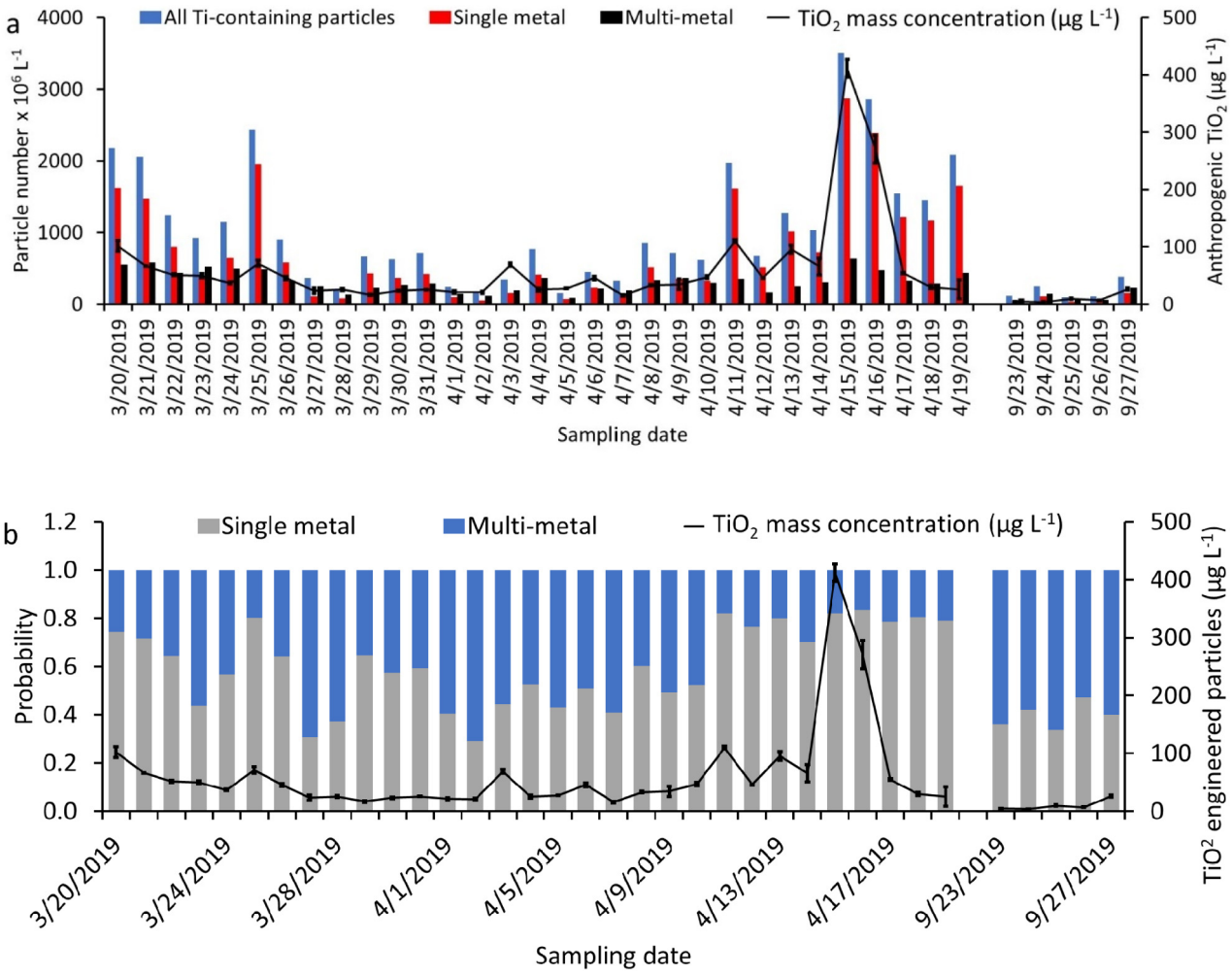


**Fig. 5.** Characterization of titanium-bearing particles by single particle-inductively coupled plasma-mass spectrometer (SP-ICP-TOF-MS): (a) number concentration of Ti-bearing particles, and (b) probability of single metal and multi-metal Ti-bearing particles.

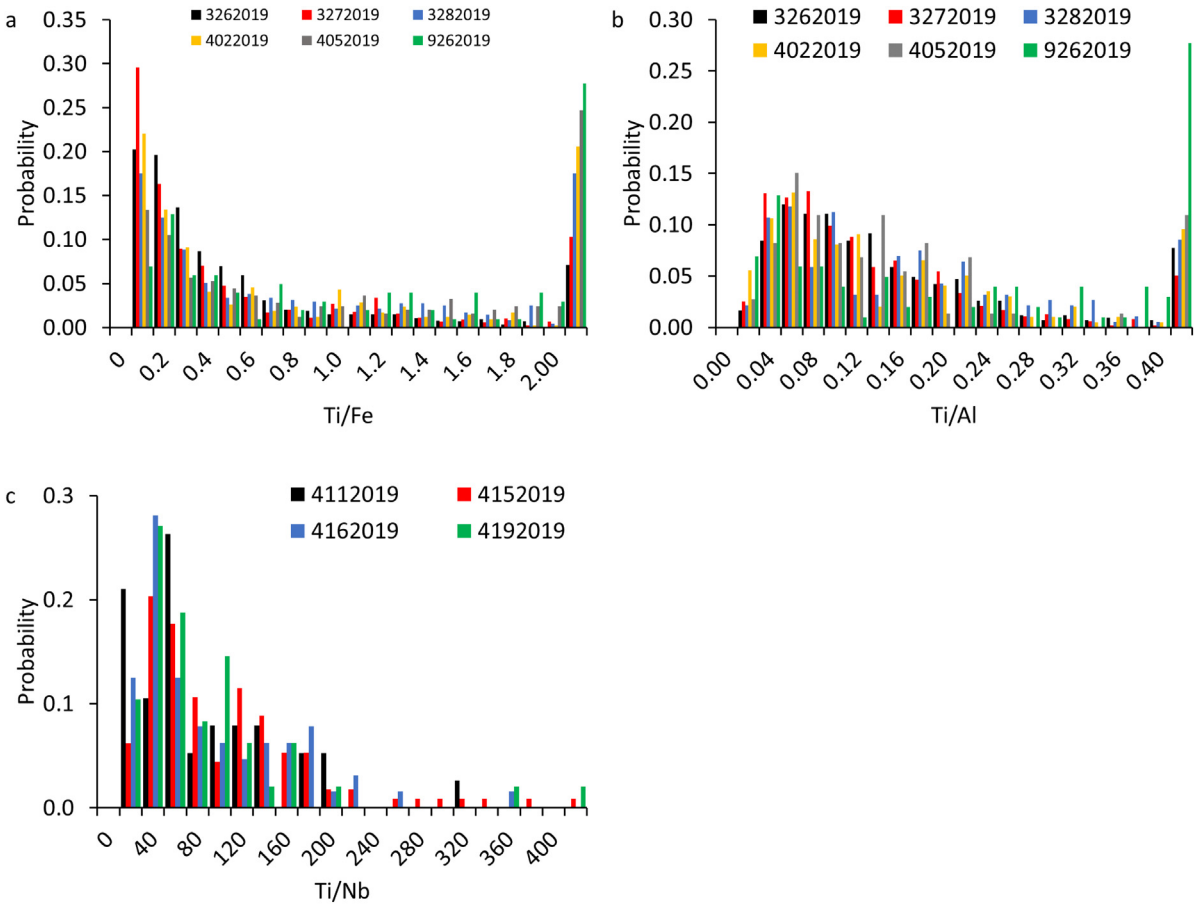


**Fig. 6.** Representative elemental ratio distribution on a single particle basis (a) Ti/Fe, (b) Ti/Al, and (c) Ti/Nb.

particles exhibited an elemental Ti/Al elemental ratio > 0.4 (2 to 28), Ti/Fe > 2.0 (15 to 25%), and Ti/Nb > 400 (0 to 3%). These elemental ratios are typical of natural Ti-bearing minerals. Ti and Fe occur in natural minerals such as: titanomagnetite ($Fe_{3-x}Ti_xO_4$, $0 < Ti/Fe < 0.43$, $0 < x < 1$) which form a complete solid solution series between end members of magnetite ($Fe_3O_4$, Ti/Fe = 0) ulvöspinel; ulvöspinel ($Fe_2TiO_4$, Ti/Fe = 0.43); pseudobrookite ($Fe_2TiO_5$, Ti/Fe = 0.43); ilmenite ($FeTiO_3$, Ti/Fe = 0.86); pseudorutile ($Fe_2Ti_3O_9$, Ti/Fe = 1.29); and ilmenorutile and ferropseudobrookite ($FeTi_2O_5$, Ti/Fe = 1.71); and iron-depleted naturally occurring Ti-particles due to weathering (*e.g.*, Ti/Fe > 2 to 20) (Baalousha et al., 2021; Weibel, 2003). Ti and Al occur in natural minerals such as: palygorskite and montmorillonite (Ti/Al = 0.014–0.016); illite (Ti/Al = 0.026); kaolinite and hectorite (Ti/Al = 0.06); vermiculite and corrensite (Ti/Al = 0.090–0.093) (Fig. 2).

Correlation coefficients between pH and Ti/Fe, probability of Ti/Fe > 2.0, and Ti/Al were calculated using Pearson's correlation method and the *p-value* for correlation was calculated using *t*-test. The elemental ratio of Ti/Fe (Fig. 7a) and the fraction of particles with Ti/Fe > 2.0 (Fig. 7b) increased with pH ($p < 0.05$). This increase in Ti/Fe on the single particle level might be attributed to the selective dissolution of Fe within Ti-bearing particles due to the increase in pH. It has been shown that Fe-Ti oxides might be subject to alteration or weathering (*e.g.*, dissolution) resulting in higher Ti/Fe elemental ratios (Weibel, 2003). For instance, the alteration of ilmenite is accomplished by the removal of structural iron, which results finally in an almost pure $TiO_2$ phase (Morad and Adin Aldahan, 1986). The alteration of ilmenite occurs through several intermediate phases, each successively enriched in titanium and depleted in iron (increasing Ti/Fe ratio), to an almost pure form of $TiO_2$ (Morad, 1986; Morad and Adin Aldahan, 1986; Mücke and Chaudhuri, 1991; Weibel, 2003). The alteration of ilmenite results in the formation of pseudorutile, fine leucoxene, and coarse leucoxene (leucoxene is a polycrystalline aggregate of rutile) (Weibel, 2003). Pseudorutile is an intermediary alteration product of ilmenite with the chemical composition $Fe_2O_3.nTiO_2.mH_2O$ ($3 < n < 5$, $1 < m < 2$) (Weibel, 2003). The elemental ratio of Ti/Al increased slightly with pH ($p < 0.05$, Fig. 7b), likely due to the lower dissolution rate of Al oxides relative to Fe oxides. The pH dependence of Ti/Fe, and Ti/Al might explain differences in estimated $TiO_2$ engineered particle concentrations based on Ti/Al, Ti/Fe, and Ti/Nb.

## 4. Conclusions and perspectives

This study provides a comprehensive approach for measuring and monitoring $TiO_2$ engineered particles in urban rivers. Total $TiO_2$ engineered particle concentrations were estimated using mass balance calculations coupled with increases in Ti/Nb, Ti/Al, and Ti/Fe elemental ratios above the natural background ratios. Single particle-inductively coupled plasma-time of flight-mass spectrometer (SP-ICP-TOF-MS) was used to characterize Ti-bearing particles at the single particle level. Furthermore, this study provides the basis for comprehensive investigation of nonpoint $TiO_2$ engineered particle release and concentrations in urban rivers during rainfall events. The elemental concentrations, $TiO_2$ concentrations, number concentration of the total-, single metal -, and multi-metal -Ti-bearing particles, and the relative abundance of single metal particles displayed temporal variability and increased with increases in runoff following rainfall events. Determining the temporal variability in engineered particle concentrations in surface waters during rainfall events is critical in improving the understanding of the environmental fate of engineered particles

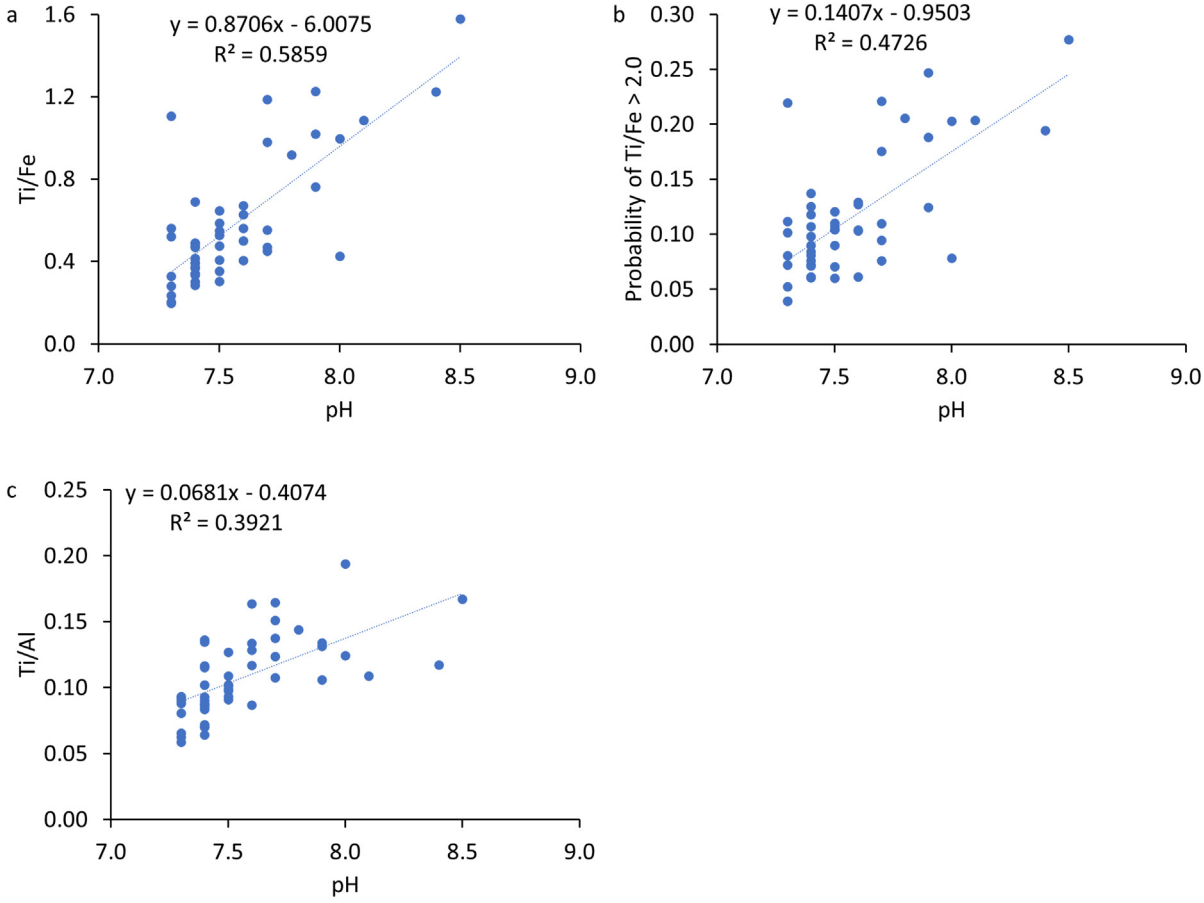


**Fig. 7.** Elemental ratio on a single particle level as a function of pH.

in surface waters and in assessing the environmental exposures to engineered particles. Elemental concentrations, ratios, and $TiO_2$ engineered particle concentrations correlated with turbidity, but not with discharge. A strong linear relationship was established between turbidity and $TiO_2$ engineered particle concentration. This relationship is important because it can be used as a substitute for the $TiO_2$ engineered particle concentration determination within the catchment area. Subsequently, this correlation is important for water resources management studies because it enables continuous monitoring of $TiO_2$ engineered particle *in situ*, which allows better understanding of $TiO_2$ engineered particle temporal behavior. Extending these findings to other sites will require parameterization of the turbidity-$TiO_2$ linear relationship as this correlation is likely to be site specific. Although turbidity measurement is cost effective and quicker than $TiO_2$ measurement, there is a need to collect higher time resolution data (*e.g.*, minutes to hours) in order to improve the understanding of the turbidity-$TiO_2$ relationship. The findings from this study can be employed to develop management strategies to control rainwater pollution at the catchment level.

## CRediT authorship contribution statement

Mr. Md Mahmudun Nabi and Dr. Jingjing Wang performed the experimental work. Dr. Goharian co-analyzed the data. Dr. Baalousha designed the field and experimental work. All authors contributed to the writing and editing of the manuscript.

## Declaration of competing interest

The authors declare no conflict of interest.

## Acknowledgment

This work was supported by US National Science Foundation CAREER (1553909) grant to Dr. Mohammed Baalousha, and by funding from the University of South Carolina, Office of Research.

## Appendix A. Supplementary data

Supplementary data to this article can be found online at https://doi.org/10.1016/j.scitotenv.2021.151081.

## References

Adamiec, E., 2017. Road environments: impact of metals on human health in heavily congested cities of Poland. Int. J. Environ. Res. Public Health 14, 697.

Azimzada, A., Jreije, I., Hadioui, M., Shaw, P., Farner, J.M., Wilkinson, K.J., 2021. Quantification and characterization of ti-, ce-, and ag-nanoparticles in global surface waters and precipitation. Environ. Sci. Technol. 55, 9836–9844.

Baalousha, M., Wang, J., Erfani, M., Goharian, E., 2021. Elemental fingerprints in natural nanomaterials determined using SP-ICP-TOF-MS and clustering analysis. Sci. Total Environ. 792, 148426.

Baalousha, M., Wang, J., Nabi, M.M., Loosli, F., Valenca, R., Mohanty, S.K., et al., 2020. Stormwater green infrastructures retain high concentrations of TiO2 engineered (nano)-particles. J. Hazard. Mater. 392, 122335.

Baalousha, M., Yang, Y., Vance, M.E., Colman, B.P., McNeal, S., Xu, J., et al., 2016. Outdoor urban nanomaterials: the emergence of a new, integrated, and critical field of study. Sci. Total Environ. 557–558, 740–753.

Chanson, H., Takeuchi, M., Trevethan, M., 2008. Using turbidity and acoustic backscatter intensity as surrogate measures of suspended sediment concentration in a small subtropical estuary. J. Environ. Manag. 88, 1406–1416.

Chen, H., Chang, H., 2014. Response of discharge, TSS, and E. Coli to rainfall events in urban, suburban, and rural watersheds. Environ Sci Process Impacts 16, 2313–2324.

Coatingsworld, 2019. U.S. Demand for Paint & Coatings to Reach 1.4 Billion Gallons in 2019.

CPC, . National weather services. Climate Prediction Center https://www.cpc.ncep.noaa.gov/ Accessed 19/4/2020.
Craigie, N., 2018. Principles of elemental chemostratigraphy. Advances in Oil and Gas Exploration & Production, Rudy Swennen. A Practical User Guide, p. 189 https://doi.org/10.1007/978-3-319-71216-1.
Daphne, L.H.X., Utomo, H.D., Kenneth, L.Z.H., 2011. Correlation between turbidity and total suspended solids in Singapore rivers. J. Water Sustain. 1, 313–322.
Gaspar, J.C., Wyllie, P.J., 1983. Ilmenite (high Mg, Mn, Nb) in the carbonatites from the Jacupiranga complex, Brazil. Am. Mineral. 68, 960–971.
Gondikas, A.P., von der Kammer, F., Reed, R.B., Wagner, S., Ranville, J.F., Hofmann, T., 2014. Release of TiO2 nanoparticles from sunscreens into surface waters: a one-year survey at the old Danube recreational lake. Environ. Sci. Technol 48, 5415–5422.
Gottschalk, F., Sun, T., Nowack, B., 2013. Environmental concentrations of engineered nanomaterials: review of modeling and analytical studies. Environ. Pollut. 181, 287–300.
Hendriks, L., Gundlach-Graham, A., Hattendorf, B., Günther, D., 2017. Characterization of a new ICP-TOFMS instrument with continuous and discrete introduction of solutions. J. Anal. At. Spectrom. 32, 548–561.
Hussain, J., Husain, I., Arif, M., Gupta, N., 2017. Studies on heavy metal contamination in godavari river basin. Appl. Water Sci. 7, 4539–4548.
Istok, J., Boersma, L., 1986. Effect of antecedent rainfall on runoff during low-intensity rainfall. J. Hydrol. 88, 329–342.
Lee, P.-K., Yu, S., Chang, H.J., Cho, H.Y., Kang, M.-J., Chae, B.-G., 2016. Lead chromate detected as a source of atmospheric pb and cr (VI) pollution. Sci. Rep. 6, 36088.
Lewis, J., 1996. Turbidity-controlled suspended sediment sampling for runoff-event load estimation. Water Resour. Res. 32, 2299–2310.
Lim, K.J., Engel, B.A., Tang, Z., Choi, J., Kim, K.S., Muthukrishnan, S., et al., 2005. Automated web GIS based hydrograph analysis tool, WHAT. J. Am. Water Res. Assoc. 41, 1407–1416.
Loosli, F., Wang, J., Rothenberg, S., Bizimis, M., Winkler, C., Borovinskaya, O., et al., 2019. Sewage spills are a major source of titanium dioxide engineered (nano)-particle release into the environment. Environ. Sci. Nano 6, 763–777.
Morad, S., 1986. SEM study of authigenic rutile, anatase and brookite in proterozoic sandstones from Sweden. Sediment. Geol. 46, 77–89.
Morad, S., Adin Aldahan, A., 1986. Alteration of detrital fe-ti oxides in sedimentary rocks. Geol. Soc. Am. Bull. 97, 567–578.
Mosbrucker, A., 2014. High resolution digital elevation model of Mount St. Helens Crater and Upper North Fork Toutle River Basin, Washington, based on an Airborne LiDAR survey of September 2009. US Department of the Interior, US Geological Survey.
Mücke, A., Chaudhuri, J.B., 1991. The continuous alteration of ilmenite through pseudorutile to leucoxene. Ore Geol. Rev. 6, 25–44.
Nabi, M.M., Wang, J., Baalousha, M., 2021a. Episodic surges in titanium dioxide engineered particle concentrations in surface waters following rainfall events. Chemosphere 263, 128261.
Nabi, M.M., Wang, J., Meyer, M., Croteau, M.-N., Ismail, N., Baalousha, M., 2021b. Concentrations and size distribution of TiO2 and ag engineered particles in five wastewater treatment plants in the United States. Sci. Total Environ. 753, 142017.
Nakashima, K., Imaoka, T., 1998. Niobian and zincian ilmenites in syenites from Cape Ashizuri, Southwest Japan. Mineral. Petrol. 63, 1–17.
Onderka, M., Krein, A., Wrede, S., Martínez-Carreras, N., Hoffmann, L., 2012. Dynamics of storm-driven suspended sediments in a headwater catchment described by multivariable modeling. J. Soils Sediments 12, 620–635.
Pace, H.E., Rogers, N.J., Jarolimek, C., Coleman, V.A., Higgins, C.P., Ranville, J.F., 2011. Determining transport efficiency for the purpose of counting and sizing nanoparticles via single particle inductively coupled plasma mass spectrometry. Anal. Chem. 83, 9361–9369.
Packman, J., Comings, K., Booth, D., 1999. Using Turbidity to Determine Total Suspended Solids in Urbanizing Streams in the Puget Lowlands.
Parker, N., Keller, A.A., 2019. Variation in regional risk of engineered nanoparticles: nanoTiO 2 as a case study. Environ. Sci. Nano 6, 444–455.
Patil, S., Barfield, B., Wilber, G., 2011. Turbidity modeling based on the concentration of total suspended solids for stormwater runoff from construction and development sites. World Environmental and Water Resources Congress 2011: Bearing Knowledge for Sustainability, pp. 477–486.
Penna, D., Tromp-van Meerveld, H., Gobbi, A., Borga, M., Dalla, Fontana G., 2011. The influence of soil moisture on threshold runoff generation processes in an alpine headwater catchment. Hydrol. Earth Syst. Sci. 15, 689–702.
Rudnick, R., Gao, S., Holland, H., Turekian, K., 2003. Composition of the continental crust. Crust 3, 1–64.
Sakson, G., Brzezinska, A., Zawilski, M., 2018. Emission of heavy metals from an urban catchment into receiving water and possibility of its limitation on the example of Lodz city. Environ. Monit. Assess. 190, 1–15.
SCdhec, 2007. Watershed Water Quality Assessment. Broad Rriver Basin., Columbia, S.C.
Sun, H., Cornish, P.S., Daniell, T., 2001. Turbidity-based erosion estimation in a catchment in South Australia. J. Hydrol. 253, 227–238.
Uhrich, M.A., Bragg, H.M., 2003. Monitoring instream turbidity to estimate continuous suspended-sediment loads and yields and clay-water volumes in the upper North Santiam River Basin, Oregon, 1998-2000. US Department of the Interior, US Geological Survey. Vol 3.
Vercruysse, K., Grabowski, R.C., 2019. Temporal variation in suspended sediment transport: linking sediment sources and hydro-meteorological drivers. Earth Surf. Process. Landf. 44, 2587–2599.
Vercruysse, K., Grabowski, R.C., Rickson, R., 2017. Suspended sediment transport dynamics in rivers: multi-scale drivers of temporal variation. Earth Sci. Rev. 166, 38–52.
Wang, J.-L., Alasonati, E., Fisicaro, P., Benedetti, M.F., 2022. Titanium nanoparticles fate in small-sized watersheds under different land-uses. J. Hazard. Mater. 422, 126695.
Wang, J., Nabi, M.M., Mohanty, S.K., Afrooz, A.N., Cantando, E., Aich, N., et al., 2020. Detection and quantification of engineered particles in urban runoff. Chemosphere 248, 126070.
Wass, P., Marks, S., Finch, J., Leeks, G.J.L., Ingram, J., 1997. Monitoring and preliminary interpretation of in-river turbidity and remote sensed imagery for suspended sediment transport studies in the humber catchment. Sci. Total Environ. 194, 263–283.
Weibel, R., 2003. Alteration of detrital fe-ti oxides in miocene fluvial deposits, Central Jutland, Denmark. Bull. Geol. Soc. Den. 50, 141–208.
Wilczyńska-Michalik, W., Rzeźnikiewicz, K., Pietras, B., Michalik, M., 2015. Fine and ultrafine TiO_ 2 particles in aerosol in Kraków (Poland). Mineralogia 45.
Zack, T., Kronz, A., Foley, S.F., Rivers, T., 2002. Trace element abundances in rutiles from eclogites and associated garnet mica schists. Chem. Geol. 184, 97–122.